OXFORD

Social Cognitive and Affective Neuroscience, 2017, 569–585

doi: 10.1093/scan/nsw169
Advance Access Publication Date: 26 December 2016
Original article

Effective amygdala-prefrontal connectivity predicts individual differences in successful emotion regulation

Carmen Morawetz,[1,4] Stefan Bode,[2] Juergen Baudewig,[3] and Hauke R. Heekeren[1,4]

[1]Department of Education and Psychology, Freie Universität Berlin, Germany, [2]Melbourne School of Psychological Sciences, The University of Melbourne, Australia, [3]Functional Imaging Unit, German Primate Center, Germany, and [4]Center for Cognitive Neuroscience Berlin, Freie Universität Berlin, Germany

Correspondence should be addressed to Carmen Morawetz, Department of Education and Psychology, Freie Universität Berlin, Habelschwerdter Allee 45, 14195 Berlin, Germany. E-mail: Carmen.morawetz@fu-berlin.de

Abstract

The ability to voluntarily regulate our emotional response to threatening and highly arousing stimuli by using cognitive reappraisal strategies is essential for our mental and physical well-being. This might be achieved by prefrontal brain regions (e.g. inferior frontal gyrus, IFG) down-regulating activity in the amygdala. It is unknown, to which degree effective connectivity within the emotion-regulation network is linked to individual differences in reappraisal skills. Using psychophysiological interaction analyses of functional magnetic resonance imaging data, we examined changes in inter-regional connectivity between the amygdala and IFG with other brain regions during reappraisal of emotional responses and used emotion regulation success as an explicit regressor. During down-regulation of emotion, reappraisal success correlated with effective connectivity between IFG with dorsolateral, dorsomedial and ventromedial prefrontal cortex (PFC). During up-regulation of emotion, effective coupling between IFG with anterior cingulate cortex, dorsomedial and ventromedial PFC as well as the amygdala correlated with reappraisal success. Activity in the amygdala covaried with activity in lateral and medial prefrontal regions during the up-regulation of emotion and correlated with reappraisal success. These results suggest that successful reappraisal is linked to changes in effective connectivity between two systems, prefrontal cognitive control regions and regions crucially involved in emotional evaluation.

Key words: PPI; fMRI; ventrolateral prefrontal cortex; reappraisal

Introduction

The ability to regulate our emotions is essential for our mental and physical well-being (Gross and Muñoz, 1995; Gross *et al.*, 2006; Eftekhari *et al.*, 2009; Berking and Wupperman, 2012). Impairment in self-regulating emotions plays a role in psychological disorders such as anxiety, major depression and several personality disorders (Davidson, 2000; Amstadter, 2008; Cisler *et al.*, 2010; Gruber *et al.*, 2012; Krause-Utz *et al.*, 2014). One well-studied emotion regulation strategy is reappraisal, which refers to the ability to cognitively change the appraisal of an emotional situation by altering its emotional impact (Gross and Thompson, 2007). Emotion regulation relies on basal cognitive functions such as working memory, attention, self-reflection, semantic memory and language (Ochsner and Gross, 2005; Zelazo and Cunningham, 2007; Phillips *et al.*, 2008), which are represented in a widespread neural network (Kalisch, 2009; Ochsner *et al.*, 2012; Buhle *et al.*, 2014; Frank *et al.*, 2014; Kohn *et al.*, 2014; Morawetz *et al.*, 2016b).

Previous research into emotion regulation has mainly used standard correlation analysis to investigate the association between activation in the cortical control network and the subcortical affective system and converged on a top-down model whereby neural responses to emotional stimuli in the amygdala and ventral striatum are down-regulated by prefrontal regions

Received: 25 April 2016; **Revised:** 27 September 2016; **Accepted:** 14 November 2016

Fig. 1. Task Design. Each trial started with an instruction screen of 2 s, showing a cue indicating the experimental condition: Red arrow pointing upwards indicated Increase, video camera indicated Look and green arrow pointing downwards indicated Decrease. The instruction was followed by the presentation of an IAPS picture for 8 s, during which subjects were asked to either up-regulate (Increase), down-regulate (Decrease) their emotions or not modulate their emotions at all (Look-Neutral, Look-Negative). After this regulation phase, subjects rated their current emotional state on a scale from 1 to 4 within 4 s. Each trial ended with a jittered fixation phase of 4–8 s.

(Ochsner and Gross, 2005; Urry *et al.*, 2006; Johnstone *et al.*, 2007; Phillips *et al.*, 2008; Wager *et al.*, 2008; Ochsner *et al.*, 2012). For example, using functional magnetic resonance imaging (fMRI), an increase in activation in the ventrolateral (Ochsner *et al.*, 2002), orbitofrontal (Ochsner *et al.*, 2004) and ventromedial prefrontal cortex (VMPFC) (Urry *et al.*, 2006) has been found to correlate with decreased amygdala activity during emotion regulation. Only few studies, however, have directly measured changes in effective connectivity during reappraisal. These further yielded inconsistent results regarding patterns of connectivity as well as proposed directions in connectivity changes (Banks *et al.*, 2007; Kanske *et al.*, 2011; Payer *et al.*, 2012; Sripada *et al.*, 2014). One possible explanation for these inconsistencies is that connectivity patterns might directly relate to individuals' reappraisal ability (i.e. regulation success), which has not been considered in most studies. Only two studies assessed emotion regulation success using behavioral self-report, but not in conjunction with effective connectivity. Using mediation analysis, one of these studies found that both ventrolateral prefrontal cortex (VLPFC) activity and reappraisal success were mediated by activity in the ventral striatum (Wager *et al.*, 2008). The second study showed that activity in the left amygdala correlated with self-reported reappraisal success (Eippert *et al.*, 2007).

We recently used dynamic causal modeling (DCM) to investigate effective connectivity during emotion regulation and demonstrated the importance of left IFG in emotion regulation (Morawetz *et al.*, 2016c). In particular, bidirectional changes in connectivity strength between the IFG and dorsolateral prefrontal cortex (DLPFC) were found to be the neural substrate of a feedback mechanism mediating reappraisal. However, as amygdala activity could not be consistently observed in each participant—which is a prerequisite for regions to be included into the DCM model space (Friston *et al.*, 2003; Lohmann *et al.*, 2012)—the amygdala could not be included in the analysis (Morawetz *et al.*, 2016c). Given that previous studies emphasized the importance of the amygdala, we aimed to expand on our findings by explicitly investigating how patterns of effective connectivity change during reappraisal in a broader network of brain regions involved in emotion regulation (including cortical and subcortical seed regions), and how these changes are linked to individuals' reappraisal success. We hypothesized that the IFG is involved in linking the prefrontal control system to regions that are directly related to basal emotion processing (such as the amygdala) in order to orchestrate emotion regulatory processes. Specifically, this study examined within-subject effective connectivity (Friston *et al.*, 1997; Friston, 2011) of the IFG and the amygdala and its association with reappraisal success using fMRI and psychophysiological interaction (PPI) analysis.

However, emotional responses not only involve changes in the brain, but also in autonomic physiology. Previous studies investigating spontaneous reactions to unpleasant pictures reported increased electrodermal activity (EDA) (Bradley *et al.*, 2008). Furthermore, reappraisal processes have been demonstrated to modulate skin conductance responses (SCRs); i.e. EDA was higher when increasing and lower when decreasing compared with maintaining emotional responses thereby indicating a modulation of emotional arousal by reappraisal (Eippert *et al.*, 2007; Urry *et al.*, 2009; Morawetz *et al.*, 2016b,c). Thus, we also recorded EDA to obtain a physiological control measure, which was expected to mirror self-reports of emotional state after emotion regulation.

Our participants were presented with highly arousing and aversive pictures while using cognitive reappraisal to increase, maintain, or decrease their emotional responses. Based on previous studies showing the involvement of the left amygdala and VLPFC in successful reappraisal (Eippert *et al.*, 2007; Wager *et al.*, 2008; Morawetz *et al.*, 2016b), we hypothesized task-dependent inter-regional covariance between the IFG and the amygdala with other brain regions that are crucially involved in emotion regulation. In addition, we were interested in how effective coupling might be dependent on reappraisal success. Since previous results were inconsistent, and no study has used cortical seed regions or included up-regulation of emotion in the experimental design, hypotheses regarding the interaction of effective coupling and regulation skills were rather unspecific. However, there are neuroanatomical studies, which demonstrated interconnections within the prefrontal cortices (Barbas and Pandya, 1989, 1991; Barbas, 2000, 2009; Goulas *et al.*, 2012; Yeterian *et al.*, 2012) and reciprocal connections between the amygdala and PFC (Amaral and Price, 1984; Ghashghaei and Barbas, 2002; Ghashghaei *et al.*, 2007). Prior neuroimaging studies also demonstrated that VLPFC and DLPFC are intrinsically connected during resting state and effectively coupled during emotion regulation (e.g. Goulas *et al.*, 2012; Morawetz *et al.*, 2016c), and similar results have been obtained for amygdala and frontal regions (e.g. Banks *et al.*, 2007; Kanske *et al.*, 2011; Ray and Zald, 2011). Based on this, we expected that (i) enhanced connectivity within the prefrontal network including lateral (VLPFC, DLPFC) and medial PFC regions (ventromedial and dorsomedial PFC; VMPFC and DMPFC) would correlate with reappraisal success, and (ii) enhanced coupling between the amygdala and PFC would predict reappraisal success.

Material and methods

Subjects

Twenty-three right-handed subjects (mean age = 25.70 years, s.d. = 5.95 years; 12 female) participated in the study. Handedness was assessed with Edinburgh-Handedness

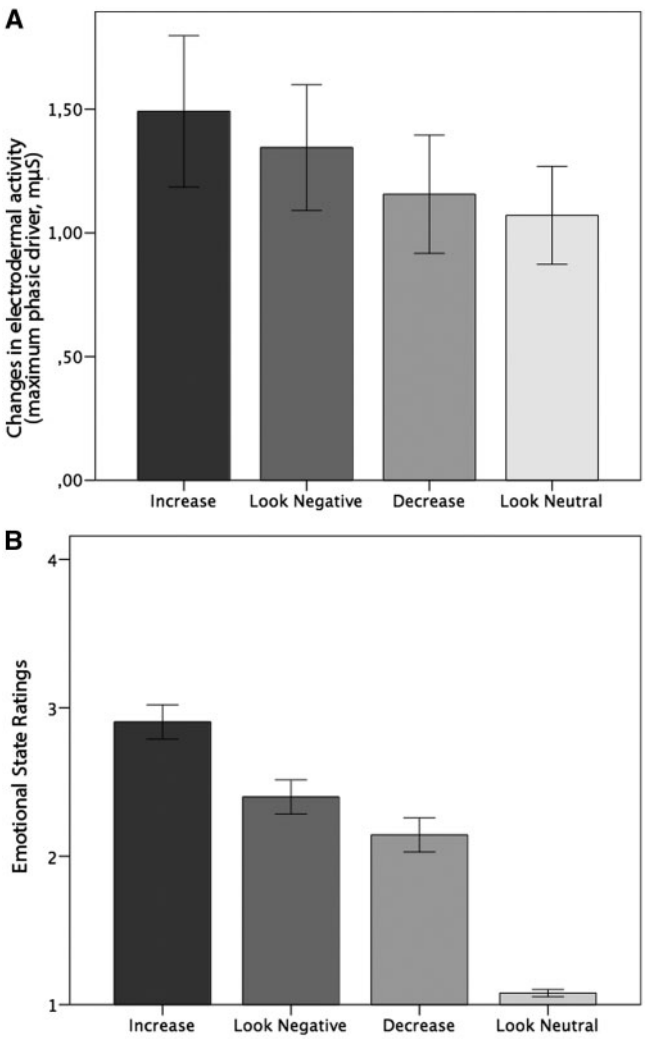

Fig. 2. (A) SCRs during scanning. Mean changes in EDA (μS) as a function of task conditions. **(B)** Emotional state ratings as a function of task conditions. After each emotion regulation phase subjects rated their current emotional state on a scale from 1 (not negative) to 4 (very negative). Error bars represent standard errors.

Inventory (Oldfield, 1971), and eligibility was assessed with a general health questionnaire and fMRI safety screening form. Subjects had normal or corrected to normal vision, gave written, informed consent to participate in the study and had no history of neurological or psychiatric disease. The study was approved by the ethics committee of the German Psychological Society and carried out in accordance to the Declaration of Helsinki.

Stimuli

Stimuli consisted of 126 aversive and 42 neutral pictures from the International Affective Picture System (IAPS) (Bradley and Lang, 2007). During the fMRI experiment, images were presented in the centre of the screen with an 800 × 600 pixel display subtending 32° × 24° visual angle on dual display goggles (VisuaStim, MR Research, USA) using the stimulation software Presentation (Version 14.1, Neurobehavioral Systems, USA). Pictures subtended a 24° × 18° visual angle, presented against a black background.

Task

The task design was adapted from previous studies (Kim and Hamann, 2007; Morawetz *et al.*, 2016b). Four task conditions were implemented (Figure 1): two reappraisal conditions ('Increase, Decrease') and two control conditions ('Look-Neutral, Look-Negative'). (i) In the 'Increase' condition, subjects were asked to engage themselves with the depicted situation and to increase their sense of subjective closeness to the displayed events by e.g. imaging a close friend/family member in the situation depicted in the picture (Ochsner *et al.*, 2004; Eippert *et al.*, 2007; Urry *et al.*, 2009). (ii) Conversely, in the 'Decrease' condition subjects were instructed to reduce the intensity of the negative emotion by distancing themselves from the image by becoming a detached observer e.g. through thinking that the depicted situation is not real. (iii) In the 'Look' condition, subjects were asked to view the neutral ('Look-Neutral') or negative ('Look-Negative') stimuli attentively and allow themselves to experience/feel any emotional responses, which these might elicit without trying to manipulate them. Subjects received a training session to practice the emotion reappraisal strategies before scanning.

Pictures were presented in an event-related design (Figure 1). Each trial started with an instruction screen (2 s) showing a symbol indicating one of the experimental conditions (camera symbol: 'Look'; red arrow pointing upwards: 'Increase'; green arrow

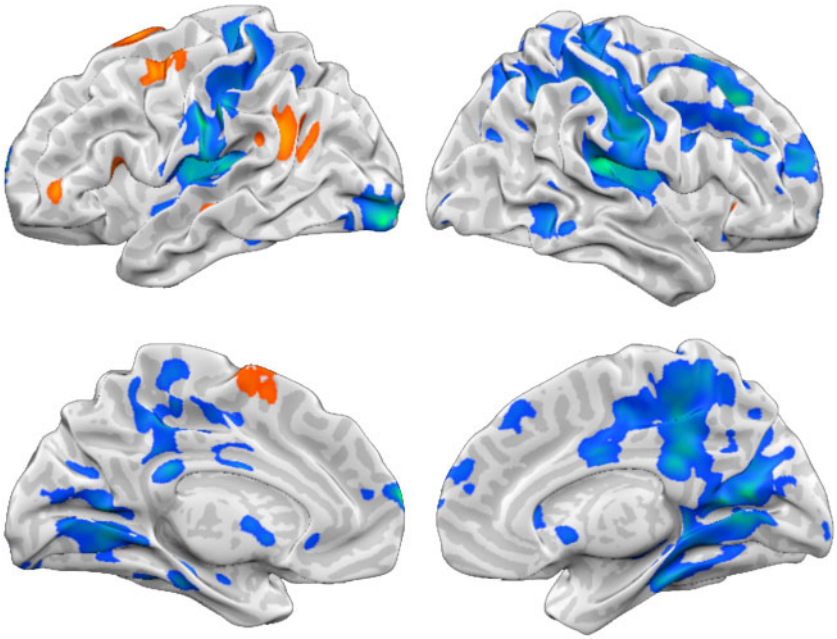

Fig. 3. Reappraisal-related activation. Reappraisal (Increase + Decrease) *vs* Look-Negative ($P < 0.05$ FEW corrected). Orange-yellow indicates stronger activity for Increase and Decrease. Blue-green indicates enhanced activity for Look-Negative.

pointing downwards: 'Decrease'). Subsequently, a picture was presented (8 s), followed by a rating of the current emotional state (4 s) (four-point Likert scale from 1 to 4; less negative to very negative). Subjects indicated their affect by pressing a button on a button fiber optic response pad (Cambridge Research Systems Ltd., England). Finally, a fixation cross presented in the centre of the screen (4–8 s) concluded the trial. One experimental run consisted of 28 trials (7 trials per condition). Each experimental session consisted of six runs (168 trials in total). Experimental conditions were randomized within runs.

Electrodermal activity

Previous research demonstrated that EDA is modulated by emotional arousal and emotion regulation (Urry *et al.*, 2009). We recorded EDA using two cup electrodes with an internal impedance of 15 kΩ (7 mm) filled with isotonic paste and attached to the proximal phalanges of the index and middle fingers on the left hand. EDA was acquired at a sampling rate of 5000 Hz using an MR-compatible amplifier system (BrainAmp GSR-module, Brain Products, Gliching, Germany) and constant voltage electrode excitation. During the analysis, the data was down-sampled offline to 10 Hz. We then decomposed skin-conductance data into continuous tonic and phasic activity (Benedek and Kaernbach, 2010a) and averaged across trials within each condition applying an 8 s time window using Ledalab Version 3.3.1 (Benedek and Kaernbach, 2010b). SCRs were defined as a deflection of at least 0.01 μS occurring 1–8 s after stimulus onset. Only runs including more than 10% SCRs exceeding the above criterion were used for analysis. Values for phasic SCRs were extracted as the difference between a local minimum and the succeeding local maximum within the response window. Due to technical problems at recording, data from seven subjects could not be analyzed, leaving a total of $n = 16$ EDA data sets.

Analysis of self-report data

As the main focus of our study was successful emotion regulation, we calculated reappraisal success scores based on the affect ratings acquired after each trial. Overall reappraisal success was defined as either the mean decrease or mean increase in reported emotion when applying a cognitive reappraisal strategy ('Increase' and 'Decrease') relative to the mean affect ratings of the control condition ('Look-Negative'), the latter representing the 'natural' emotional response to the stimuli. The 'Look-Neutral' condition served mainly as a break in the task design in which no emotions were elicited. Thus, reappraisal success scores for 'Increase' ('Increase' minus 'Look-Negative') and 'Decrease' ('Decrease' minus 'Look-Negative') for each participant were used as a predictor in the PPI analysis.

fMRI data acquisition

Whole brain functional and anatomical images were acquired using a 3.0 T Magnetom TrioTim MRI scanner (Siemens, Erlangen, Germany) with a 12-channel head coil. A high-resolution 3D T1-weighted dataset was acquired for each subject (176 sagittal sections, $1 \times 1 \times 1$ mm^3; 256×256 data acquisition matrix). Functional images were acquired using a T2*-weighted, gradient-echo planar imaging pulse sequence recording 37 sections oriented parallel to the anterior and posterior commissure at an in-plane resolution of $3 \times 3 \times 3$mm^3 (interslice gap = 0; TE = 30 ms; TR = 2 s; FA = 90°; FoV = 192×192 mm^2; 64×64 data acquisition matrix). For each experimental run 285 whole brain volumes were recorded.

fMRI data analysis

Data were analyzed using a random effects general linear model (GLM) as implemented in BrainVoyager QX 2.3.1 (Brain Innovation, Maastricht, The Netherlands). Pre-processing of fMRI data included 3D-motion-correction, temporal high pass

Table 1. Effects of reappraisal

Region	BA	Side	Coordinates			Voxels	t-value
			x	y	z		
'Increase+Decrease>Look Negative'							
Superior Frontal Gyrus*	6	LH	−15	11	70	197	4.11
SFG	6	LH	−15	11	70	LM	4.11
medFG	6	LH	−9	2	61	LM	2.96
STG	39	LH	−45	−52	28	234	3.96
MFG	6	LH	−39	−1	64	162	3.93
IFG	13	LH	−45	26	7	186	3.75
IFG	13	LH	−45	26	7	LM	3.75
'Look Negative > Increase + Decrease'							
medFG	10	LH	−6	65	16	11306	6.10
Insula	13	LH	−45	−13	7	LM	5.95
Post-central gyrus	2	LH	−57	−22	31	LM	5.61
Transverse temporal gyrus	41	LH	−42	−31	13	LM	5.29
SFG	9	RH	42	35	25	LM	5.27
Posterior cingulate	30	RH	12	−61	10	LM	5.25
MFG	8	RH	24	11	40	LM	5.25
Post-central gyrus	40	LH	−63	−19	19	LM	5.23
Insula	13	LH	−27	−28	16	LM	5.19
Insula	13	RH	33	−22	19	LM	5.06
Precuneus	7	RH	24	−61	34	LM	4.98
Post-central gyrus	2	RH	51	−28	40	LM	4.96
medFG	8	RH	18	29	43	LM	4.95
Pre-central gyrus	6	RH	48	−10	22	LM	4.84
Inferior parietal lobule	40	RH	36	−34	46	LM	4.79
Inferior parietal lobule	40	RH	54	−28	22	LM	4.51
MFG	6	RH	27	14	61	LM	4.32
Lingual gyrus	19	LH	−15	−61	4	LM	4.29
Lentiform nucleus		RH	33	−13	4	LM	4.29
medFG	6	RH	15	−13	49	LM	4.15
Paracentral lobule	5	RH	12	−37	46	LM	4.15
SFG	10	RH	27	53	16	LM	4.09
Cingulate gyrus	31	RH	3	−37	31	LM	4.08
Paracentral lobule	4	RH	9	−37	58	LM	3.83
SFG	10	RH	9	68	13	LM	3.82
Post-central gyrus	2	LH	−24	−34	67	LM	3.80
Cingulate gyrus	24	LH	0	−4	31	LM	3.73
Inferior temporal gyrus	20	RH	54	−46	−11	LM	3.68
Caudate		LH	−6	8	−2	LM	3.55
Superior parietal lobule	7	LH	−27	−52	43	LM	3.53
Precuneus	31	LH	−24	−67	22	LM	3.50
Lentiform nucleus		RH	24	−1	−2	LM	3.46
Post-central gyrus	3	RH	30	−31	61	LM	3.37
Inferior parietal lobule	40	LH	−42	−37	40	LM	3.36
Post-central gyrus	43	RH	66	−13	16	LM	3.31
medFG	9	RH	15	41	19	LM	3.29
Parahippocampal gyrus	28	RH	27	−22	−5	LM	3.28
Sub−gyral	40	LH	−21	−34	55	LM	3.26
Fusiform gyrus	37	LH	−51	−43	−17	LM	3.22
Cingulate gyrus	24	RH	9	−13	40	LM	3.21
Pre-central gyrus	9	RH	45	17	34	LM	3.21
Insula	13	LH	−39	−1	−8	LM	3.20
Fusiform gyrus	37	LH	−39	−58	−8	LM	3.16
Middle temporal gyrus	19	RH	33	−61	10	LM	3.16
Caudate		RH	15	23	7	LM	3.06
Middle temporal gyrus	21	RH	66	−7	−2	LM	3.01
Caudate		RH	9	11	−2	LM	3.00
STG	22	LH	−66	−19	1	LM	2.96
Cingulate gyrus	31	LH	−15	−25	34	LM	2.91
medFG	6	LH	−9	−16	46	LM	2.89
medFG	9	RH	6	50	25	LM	2.87
Cingulate gyrus	24	LH	−12	−7	46	LM	2.61

(continued)

Table 1. (continued)

Region	BA	Side	Coordinates			Voxels	t-value
			x	y	z		
Cuneus	18	LH	−18	−79	22	LM	2.60
medFG	10	LH	−9	47	13	LM	2.47
Precuneus	7	RH	6	−58	37	LM	2.46
Middle occipital gyrus	19	RH	30	−79	13	LM	2.32
Thalamus		RH	15	−22	4	LM	2.28
Inferior occipital gyrus	18	LH	−33	−97	−11	379	5.57
Parahippocampal gyrus	36	LH	−33	−28	−17	131	4.22

LM, local maxima.

filtering (three cycles/run), linear trend removal, slice scan time correction, spatial smoothing (Gaussian smoothing kernel, 8 mm full width half maximum), and transformation into Talairach space (Talairach and Tournoux, 1988).

Data were visualized and statistically thresholded using NeuroElf Version 0.9c (neuroelf.net). We utilized height and cluster size thresholding after establishing family wise error (FWE) thresholds using the alphasim procedure (Forman *et al.*, 1995) at an initial significance level of $P < 0.001$ and an FWE cluster level correction of $P < 0.05$ (implemented in NeuroElf, http://neuroelf.net). AlphaSim was computed for each map separately so as to accurately estimate the inherent smoothness of each contrast, rather than to rely on the size of the Gaussian kernel used during pre-processing which can lead to errors in thresholding (Bennett *et al.*, 2009). Extent thresholds for the contrasts of the univariate analysis were thresholded at 95 voxels and PPI maps were thresholded at 91 voxels.

Univariate analysis. Separate regressors in the GLM were specified for the instruction cue, rating, and the conditions during stimulus viewing. The regressors-of-interest were the four task conditions 'Increase, Decrease, Look-Negative and Look-Neutral'. The 'Look-Negative' condition constituted the natural response to all images and was used as a control condition. As described below, emotion regulation contrasts were defined as 'differences' to this control condition.

In line with our a priori hypotheses, we used the left IFG and amygdala as regions of interest (ROIs). The left IFG and the amygdala were chosen as ROIs and seed regions for the PPI analyses on the basis of the following three criteria: (i) Prior evidence of their functional involvement in emotion regulation tasks: Several meta-analyses have implicated both regions in emotion regulation (Kalisch, 2009; Diekhof *et al.*, 2011; Ochsner *et al.*, 2012; Buhle *et al.*, 2014; Frank *et al.*, 2014; Kohn *et al.*, 2014; Messina *et al.*, 2015). Amygdala activity has been associated with emotion processing, emotional reactivity and the evaluation of emotional stimuli (Phan *et al.*, 2002; Zald, 2003 ; Sergerie *et al.*, 2008; Ray and Zald, 2012). The VLPFC is known to be implicated in emotion regulation processes such as in the semantic description of emotional states and in response selection/inhibition (Phillips *et al.*, 2008; Ochsner *et al.*, 2012; Ray and Zald, 2012). Furthermore, recent meta-analyses support the view that the VLPFC/IFG is involved in language and semantic processes during emotion regulation (Kohn *et al.*, 2014; Messina *et al.*, 2015). In line with these findings, one of our previous studies indicated a key role of the left IFG within the emotion regulation network (Morawetz *et al.*, 2016a). (i) Prior evidence for an association between reappraisal success and brain activity in those regions: Increased activity in left IFG and the amygdala have been associated with reappraisal success (Eippert *et al.*, 2007; Morawetz *et al.*, 2016a,b; Wager *et al.*, 2008). (ii) Evidence in our own fMRI study for task effects in those regions: Our whole-brain analysis revealed significant task-related effects of emotion regulation in the left IFG, but not within the amygdala. Thus, based on the contrast ('Increase + Decrease > Look-Negative'), we functionally determined the left IFG, which was subsequently used as seed region (left IFG: −45, 26, 7; 5022 mm^3), while the amygdala was defined purely anatomically using the Anatomy Toolbox (Eickhoff *et al.*, 2005) (left amygdala: −18, −4, −16; 1546 mm^3; right amygdala: 22, −3, −15, 1424 mm^3). Furthermore, we performed an ROI analysis of the bilateral amygdala to demonstrate reappraisal-related activity (see 'Results' section and Supplementary Figure S1).

PPI analysis. To compare changes in effective coupling between different brain regions (physiological component) during reappraisal and passive looking (psychological component) we performed an analysis of PPI (Friston *et al.*, 1997) using NeuroElf.

Our PPI analysis was based on the two ROI regions, the left IFG and the left amygdala (see above). Time-series from the left amygdala and left IFG were extracted as physiological seeds by averaging the neural activity within single-subject ROI masks, and the regulation contrasts ('Increase > Look-Negative') and ('Decrease > Look-Negative') were used as psychological context, to create the PPI term. This interaction term was entered into a voxelwise regression, with the covariates of amygdala and IFG raw time-series and all original regressors of the GLM model (Instruction, Rating, 'Increase, Decrease, Look-Negative, Look-Neutral'). The resulting PPI parameter estimates denoted the change in strength of effective coupling between the seed regions and the remainder of the brain during reappraisal relative to 'Look-Negative' trials (see Supplementary Tables S1 and S2). To examine the extent to which individual differences in reappraisal ability predicted this connectivity, reappraisal success scores were entered as a covariate into a voxelwise regression, serving as a predictor of the PPI map.

Results

Behavioral results

Emotion induction. Skin conductance data provided support for the success of the emotion induction (Figure 2A). We found a significant main effect of task [$F(1,15) = 3.80$, $P < 0.01$]. *Post-hoc* t-tests indicated that SCRs during 'Increase' were higher compared with 'Decrease' [$t(15) = 2.62$, $P < 0.05$] and 'Look-Neutral' [$t(15) = 2.78$, $P < 0.05$]. The SCR amplitudes were significantly higher during the 'Look-Negative' compared with the 'Look-Neutral' condition [$t(15) = 2.35$, $P < 0.05$].

Emotion regulation. A significant main effect of task was found [$F(1,22) = 50.92$, $P < 0.001$] (Figure 2B). *Post-hoc* t-tests

Table 2. Effects of down-regulation of emotion

Region	BA	Side	Coordinates			Voxels	t-value
			x	y	z		
'Decrease>Look Negative'							
IFG	45	LH	−45	23	10	164	3.94
IFG	45	LH	−45	38	1	LM	2.71
SFG	6	LH	−12	11	67	145	3.79
SFG	6	LH	−9	−1	73	LM	2.65
STG	22	LH	−51	−55	19	161	3.61
'Look Negative >Decrease'							
medFG	10	LH	−6	65	16	12716	7.35
Inferior occipital gyrus	18	LH	−33	−97	−11	LM	6.13
Insula	13	RH	33	−25	19	LM	6.03
Pre-central gyrus	6	RH	48	−10	25	LM	5.82
post-central gyrus	40	LH	−63	−22	19	LM	5.70
Inferior parietal lobule	40	RH	57	−28	22	LM	5.48
Caudate		LH	−9	20	13	LM	5.46
Post-central gyrus	2	LH	−57	−22	31	LM	5.23
Insula	13	LH	−30	−31	16	LM	5.19
Post-central gyrus	2	RH	36	−25	31	LM	5.11
Insula	41	LH	−45	−25	16	LM	4.86
Post-central gyrus	2	LH	−24	−37	67	LM	4.71
Cuneus	23	RH	15	−70	10	LM	4.57
Posterior cingulate	30	LH	−12	−61	13	LM	4.56
Cingulate gyrus	31	LH	−21	−40	37	LM	4.51
Caudate		LH	−3	11	7	LM	4.50
Cingulate gyrus	32	RH	18	20	31	LM	4.47
Caudate		RH	36	−34	−5	LM	4.40
Cingulate gyrus	24	RH	18	8	28	LM	4.29
Posterior cingulated	30	LH	−21	−52	10	LM	4.29
medFG	6	LH	−12	−7	49	LM	4.19
Posterior cingulate	30	RH	30	−61	10	LM	4.16
Caudate		RH	15	26	7	LM	4.15
Parahippocampal gyrus	27	RH	9	−37	4	LM	4.12
Precuneus	7	RH	24	−61	34	LM	4.09
MFG	8	RH	24	20	43	LM	4.07
Insula	13	LH	−45	−7	10	LM	4.05
Paracentral lobule	5	LH	−6	−37	49	LM	4.02
Cingulate gyrus	31	LH	−15	−25	37	LM	4.01
Inferior parietal lobule	40	RH	36	−34	46	LM	3.97
SFG	9	RH	39	35	25	LM	3.97
medFG	6	RH	12	−13	49	LM	3.89
Post-central gyrus	2	RH	51	−25	40	LM	3.88
Parahippocampal gyrus	36	LH	−36	−28	−17	LM	3.88
Post-central gyrus	5	RH	27	−40	64	LM	3.88
Cingulate gyrus	31	RH	15	−22	37	LM	3.88
Parahippocampal gyrus	35	LH	−24	−25	−23	LM	3.84
Insula	13	LH	−39	−1	−8	LM	3.81
Cingulate gyrus	31	LH	0	−43	34	LM	3.79
Post-central gyrus	3	LH	−9	−34	64	LM	3.74
Paracentral lobule	4	RH	9	−37	58	LM	3.72
Anterior cingulate	32	LH	−3	47	1	LM	3.71
Precuneus	7	RH	9	−34	43	LM	3.71
Post-central gyrus	7	RH	6	−52	67	LM	3.66
Pre-central gyrus	4	RH	18	−28	64	LM	3.66
Parahippocampal gyrus	30	RH	21	−49	10	LM	3.66
medFG	10	RH	15	47	13	LM	3.55
Cuneus	18	RH	15	−100	−2	LM	3.51
Inferior Parietal Lobule	40	LH	−45	−34	37	LM	3.48
Precuneus	19	LH	−30	−67	31	LM	3.46
Cingulate Gyrus	32	RH	24	8	43	LM	3.46
Cingulate Gyrus	31	RH	27	−49	25	LM	3.43
Middle Occipital Gyrus	18	LH	−27	−79	1	LM	3.41
Caudate		RH	33	−43	10	LM	3.39

(continued)

Table 2. (continued)

Region	BA	Side	Coordinates			Voxels	t-value
			x	y	z		
Posterior cingulate	29	RH	3	−52	13	LM	3.38
Lentiform nucleus		RH	21	−1	−2	LM	3.37
Pre-central gyrus	6	LH	−57	−1	10	LM	3.23
Middle occipital gyrus	18	RH	33	−94	1	LM	3.17
Lingual gyrus	17	RH	12	−97	−14	LM	3.13
Cingulate gyrus	24	LH	0	−4	31	LM	3.06
Cingulate gyrus	24	LH	−15	5	31	LM	2.95
Caudate		LH	−24	−10	25	LM	2.91
Cuneus	18	RH	3	−85	19	LM	2.83
Inferior occipital gyrus	17	RH	27	−100	−11	LM	2.69
medFG	9	RH	6	47	28	LM	2.69
Fusiform gyrus	19	RH	27	−61	−8	LM	2.65
MFG	6	RH	27	14	61	LM	2.62
Precuneus	7	LH	−6	−64	64	LM	2.60
MFG	10	RH	48	50	13	LM	2.57
Precuneus	7	RH	27	−58	49	LM	2.54
Parahippocampal gyrus	28	RH	15	−10	−11	LM	2.53
Parahippocampal gyrus	19	RH	24	−52	−5	LM	2.49
fusiform gyrus	19	LH	−24	−64	−8	LM	2.46
Precuneus	7	RH	12	−67	46	LM	2.44
Cuneus	18	LH	−21	−79	22	LM	2.27

LM, local maxima.

revealed significantly more negative emotional state ratings for 'Increase' compared with 'Decrease [$t(22) = 9.25$, $P < 0.001$], as well as for 'Increase' compared with 'Look-Negative' [$t(22) = 6.13$, $P < 0.001$] and 'Look-Neutral' [$t(22) = 16.24$, $P < 0.001$]'. 'Look-Negative' also resulted in more negative emotional state ratings compared with 'Decrease' [$t(22) = 3.98$, $P < 0.01$] and compared with 'Look-Neutral' [$t(22) = 12.20$, $P < 0.001$]. 'Decrease' was associated with higher emotional state ratings as 'Look-Neutral' [$t(22) = 9.88$, $P < 0.001$]. These results confirm that emotion regulation was successful.

fMRI data

General effects of reappraisal. First, we tested for reappraisal effects independent of reappraisal goals by contrasting ['Increase + Decrease > Look-Negative'] (Figure 3, Table 1). Reappraisal was associated with increased responses in prefrontal regions including superior frontal (SFG), medial frontal (medFG), middle frontal (MFG) and IFG as well as superior temporal gyrus (STG).

The contrast 'Decrease' compared with 'Look-Negative' revealed increased activity in left IFG, SFG, and STG (Table 2). The contrast between 'Increase' and 'Look-Negative' revealed enhanced responses in left MFG, SFG, IFG, STG and pre-central gyrus (Table 3).

Univariate ROI analyses. Based on our *a priori* hypotheses, we performed ROI analyses on bilateral amygdala by calculating the mean signal change across all voxels within the ROI (Supplementary Figure S1). This analysis was conducted to provide evidence of activity related to emotion regulation i.e. either differential activity between 'Increase' and 'Decrease', or between 'Decrease' and 'Look-Negative/Look-Neutral', or 'Increase' and 'Look-Negative/Look-Neutral', supporting the applicability of the following PPI analysis in these regions.

A main task effect was observed in the left amygdala [$F(1,22) = 3.08$, $P < 0.05$], but not within the right amygdala. *Post-hoc* tests revealed that responses in the left amygdala significantly differed between the 'Increase' and 'Decrease' condition [$t(22) = 2.72$, $P < 0.05$]. Thus, the left amygdala was used as seed region in the subsequent PPI analyses.

Effective connectivity analysis. We applied a seed-based connectivity analysis to examine changes in effective connectivity during emotion regulation relative to the 'Look-Negative' condition with respect to reappraisal skills (ability to successfully regulate emotions, as measured by the reappraisal success scores). PPI analyses were performed on two seed regions, left IFG and left amygdala. For this, we determined task-dependent effective interaction based on the contrast 'Increase' or 'Decrease' *vs* control condition ('Increase > Look-Negative' and 'Decrease > Look-Negative') using the individual mean reappraisal success scores as predictor of the PPI map, meaning that the better subjects could regulate their emotions, the stronger was the effective coupling between the seed regions and the remainder of the brain. A positive correlation means that the greater the task-dependent change in effective connectivity between these regions and the seed region, the more effectively participants regulated their emotions during the 'Increase' or 'Decrease' condition. Contrarily, a negative correlation means that a greater task-dependent change in effective connectivity between these regions and the seed region was associated with less effective emotion regulation during the 'Increase' or 'Decrease' condition.

Left IFG seed region. During the up-regulation of emotion we found a positive correlation between 'Increase' success and the effective coupling of the left IFG (seed region) and left STG, VMPFC and bilateral amygdalae (Table 4; Figure 4A illustrates one of these positive correlations, using the success-dependent connectivity between IFG as seed region and the left amygdala). We also observed a negative correlation between 'Increase' success and activity of the left IFG that was coupled with pregenual anterior cingulate cortex (pgACC), DMPFC, caudate, right insula,

Table 3. Effect of up-regulation of emotion

Region	BA	Side	Coordinates			Voxels	t-value
			x	y	z		
'Increase>Look Negative'							
STG	13	LH	−42	−46	25	234	4.66
MFG	6	LH	−36	−1	61	351	4.15
SFG	6	LH	−6	11	73	LM	3.74
SFG	6	LH	−6	−4	64	LM	3.09
IFG	45	LH	−47	37	4	175	3.41
IFG	45	LH	−49	22	11	LM	2.85
IFG	44	LH	−47	4	14	LM	2.46
Insula	13	LH	−35	0	14	LM	2.36
'Look Negative>Increase'							
Post-central gyrus	1	RH	66	−16	28	6174	7.02
medFG	8	RH	15	29	43	LM	5.98
Cingulate gyrus	32	RH	24	8	40	LM	5.01
Precuneus	19	RH	30	−61	40	LM	4.94
Post-central gyrus	3	RH	33	−34	46	LM	4.61
MFG	6	RH	24	11	61	LM	4.59
Lentiform nucleus		RH	33	−13	4	LM	4.48
Posterior cingulate	30	RH	12	−61	10	LM	4.48
Post-central gyrus	2	RH	51	−25	40	LM	4.36
MFG	46	RH	42	35	22	LM	4.24
Pre-central gyrus	9	RH	45	17	34	LM	4.23
Insula	13	RH	30	−22	19	LM	4.02
Lingual gyrus	19	LH	−15	−58	−2	LM	4.01
Insula	13	RH	39	−28	13	LM	3.96
Cingulate gyrus	31	RH	3	−37	31	LM	3.83
Inferior temporal gyrus	20	RH	51	−49	−11	LM	3.78
Paracentral lobule	5	RH	9	−37	46	LM	3.61
Cingulate gyrus	24	RH	3	−1	31	LM	3.56
Lingual gyrus	19	RH	15	−46	−2	LM	3.52
STG	41	RH	54	−19	10	LM	3.50
Parahippocampal gyrus	36	RH	33	−28	−23	LM	3.43
Paracentral lobule	5	LH	0	−43	61	LM	3.36
Post-central gyrus	3	RH	33	−31	61	LM	3.15
Inferior parietal lobule	40	RH	57	−46	49	LM	2.79
medFG	6	LH	−6	−19	49	LM	2.73
Middle occipital gyrus	37	RH	39	−61	4	LM	2.26
STG	22	LH	−48	−13	7	1253	5.26
Post-central gyrus	2	LH	−60	−22	34	LM	4.70
Post-central gyrus	40	LH	−63	−19	19	LM	4.43
STG	41	LH	−42	−34	13	LM	4.20
Insula	13	LH	−33	−19	19	LM	3.85
Inferior parietal lobule	40	LH	−48	−28	46	LM	3.59
STG	22	LH	−66	−19	1	LM	3.33
Superior parietal lobule	7	LH	−27	−55	46	LM	3.32
IFG	9	LH	−63	8	31	LM	2.84
Post-central gyrus	5	LH	−30	−40	58	LM	2.66
Post-central gyrus	2	LH	−24	−34	67	LM	2.64
MFG	10	RH	27	62	22	LM	4.04
MFG	10	RH	27	62	22	LM	4.04
SFG	10	RH	9	68	13	LM	3.61
SFG	10	LH	−9	65	16	LM	3.37
SFG	10	RH	3	65	28	LM	2.52
medFG	9	RH	6	50	28	LM	2.48
Parahippocampal gyrus	36	LH	−33	−28	−17	303	4.02
Fusiform gyrus	37	LH	−42	−58	−8	LM	3.61
Fusiform gyrus	37	LH	−48	−46	−14	LM	3.08
Middle occipital gyrus	19	LH	−57	−67	−5	LM	2.99
Middle temporal gyrus	21	LH	−66	−55	4	LM	2.77
STG	22	LH	−63	−61	16	LM	2.75
Middle occipital gyrus	19	LH	−51	−82	10	250	3.72
Fusiform gyrus	18	LH	−27	−97	−17	LM	3.61
STG	38	RH	48	17	−20	102	3.31
IFG	47	RH	36	20	−14	LM	3.23

LM, local maxima.

Table 4. Task-related PPI analysis with success scores as covariate for left IFG seed region

Region	BA	Side	Coordinates			Voxels	t-value
			x	y	z		
'Decrease > Look Negative with Decrease success as covariate'							
Middle temporal gyrus	21	RH	39	−4	−23	173	0.70
Middle temporal gyrus	21	RH	39	−4	−23	LM	0.70
STG	22	RH	51	−16	−8	LM	0.61
STG	38	RH	42	5	−11	LM	0.59
STG	38	RH	57	14	−11	LM	0.54
SFG/DMPFC	10	LH	−27	44	16	148	0.63
SFG	10	LH	−27	44	16	LM	0.63
medFG	10	LH	−9	50	10	LM	0.61
IFG/VMPFC	11	RH	18	35	−17	155	−0.69
IFG	11	RH	18	35	−17	LM	−0.69
IFG	47	RH	21	23	−17	LM	−0.62
SFG	11	LH	−12	44	−14	100	−0.62
Orbital Gyrus	47	LH	−15	20	−23	95	−0.59
Orbital gyrus	47	LH	−15	20	−23	LM	−0.59
Subcallosal gyrus	25	LH	−3	8	−14	LM	−0.56
Lentiform nucleus/putamen		LH	−21	5	16	171	0.68
Lentiform nucleus/putamen		LH	−21	5	16	LM	0.68
MFG	8	LH	−30	20	37	LM	0.65
MFG/DLPFC	9	LH	−42	14	37	LM	0.55
Pre-central Gyrus/DLPFC	9	LH	−33	5	34	LM	0.52
'Increase>Look Negative with Increase success as covariate'							
Uncus	20	LH	−24	−7	−41	184	0.66
STG	38	LH	−30	8	−20	LM	0.59
Parahippocampal gyrus (amygdala)		LH	−24	−7	−17	LM	0.52
Parahippocampal gyrus (amygdala)	34	RH	27	5	−14	138	0.62
IFG/VMPFC	47	RH	26	17	−11	LM	0.57
Anterior cingulate	32	LH	−12	38	10	1146	−0.83
Cingulate gyrus	24	LH	−9	14	25	LM	−0.72
Cingulate gyrus	24	LH	−6	5	25	LM	−0.67
medFG/DMPFC	10	RH	15	53	13	LM	−0.70
medFG/DMPFC	10	LH	0	56	16	LM	−0.54
Anterior cingulate/DMPFC	32	RH	12	35	16	LM	−0.62
Cingulate gyrus/DMPFC	32	RH	9	20	34	LM	−0.54
Caudate		LH	−6	23	7	LM	−0.70
Insula	13	RH	33	29	10	LM	−0.52
Caudate		LH	−12	8	4	LM	−0.52
Fusiform gyrus	18	LH	−24	−100	−14	151	−0.69
Cingulate gyrus	24	LH	−9	−7	37	679	−0.69
Cingulate gyrus	31	RH	6	−34	34	LM	−0.66
Cingulate gyrus	31	RH	9	−22	40	LM	−0.62
Cingulate gyrus	24	RH	9	−4	37	LM	−0.60
Cingulate gyrus	31	LH	−18	−46	25	LM	−0.60
Cingulate gyrus	31	RH	24	−22	40	LM	−0.59
medFG	6	RH	9	−16	58	LM	−0.58
Cingulate gyrus	31	LH	−18	−28	37	LM	−0.57
Inferior parietal lobule	40	LH	−30	−37	37	LM	−0.56
Precuneus	31	RH	9	−46	34	LM	−0.54
Paracentral lobule	6	LH	−6	−25	52	LM	−0.53
Paracentral lobule	5	RH	21	−34	49	LM	−0.50
MFG	47	RH	51	41	−8	119	−0.67
STG	38	RH	54	20	−14	LM	−0.67
IFG	46	RH	51	41	13	LM	−0.59
Cuneus	19	RH	30	−88	28	239	−0.65
Cuneus	19	RH	12	−91	25	LM	−0.59
Pre-central gyrus	6	RH	57	2	37	177	−0.65
Middle temporal gyrus	21	RH	66	−4	−5	LM	−0.62
STG	42	RH	69	−10	7	LM	−0.58
IFG	44	RH	57	8	16	LM	−0.56
STG	22	RH	60	2	4	LM	−0.53
STG	22	RH	48	−10	−2	LM	−0.54

LM, local maxima.

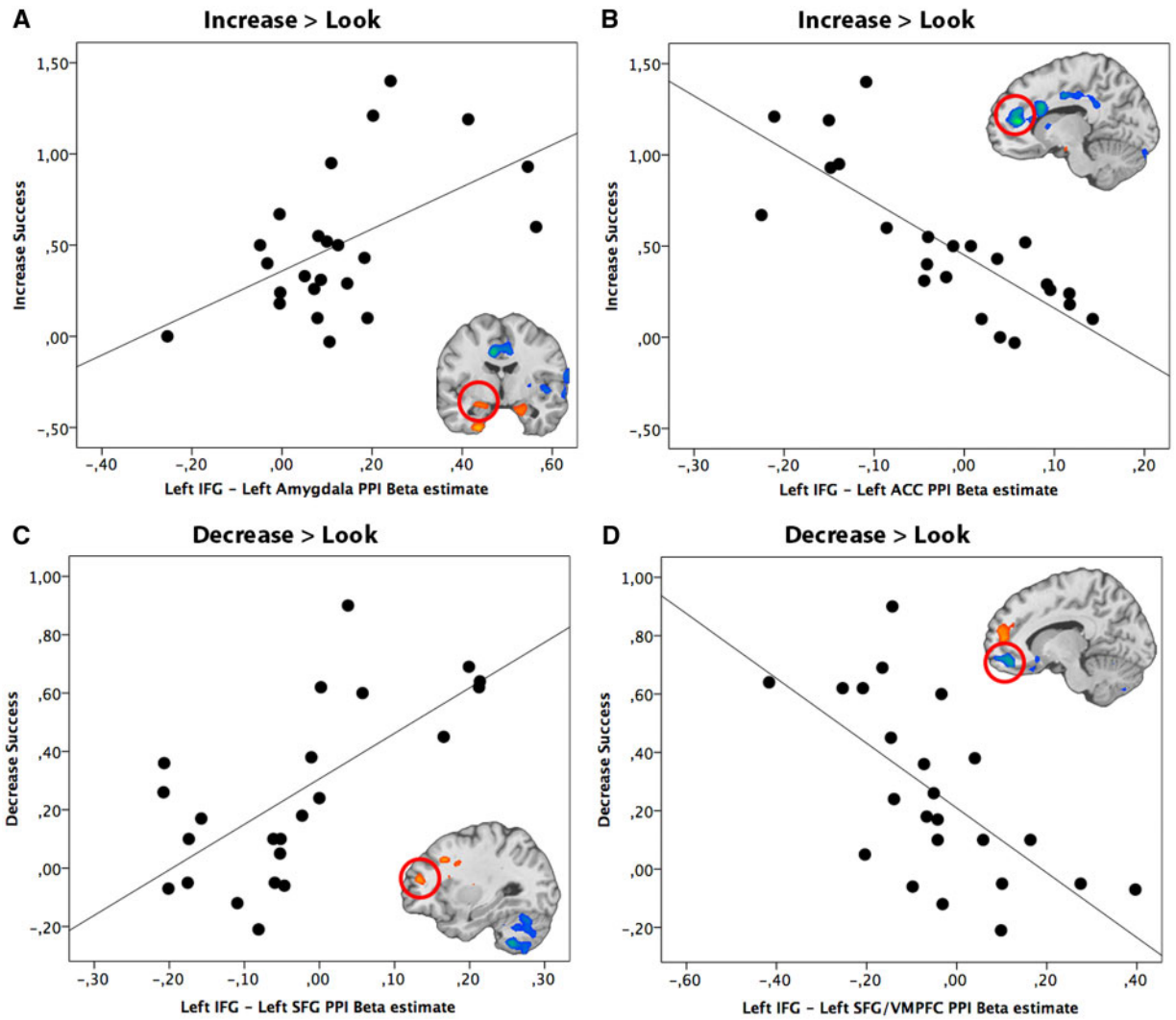

Fig. 4. Relationship between reappraisal success scores (Increase Success) and PPI beta estimate of IFG coupling with **(A)** left amygdala and **(B)** left ACC during the upregulation of emotion (Increase > Look). Relationship between reappraisal success (Decrease Success) scores and PPI beta estimate of IFG coupling with **(C)** left (SFG/DMPFC) and **(D)** left (SFG/VMPFC) during the down-regulation of emotion (Decrease > Look). The scatter plot is solely for illustrative purposes (e.g. to show the absence of outliers), and is not used for statistical inference.

left IPL, right MFG, right STG and right IFG (Table 4). Figure 4B illustrates the negative correlation between 'Increase' success and connectivity between left IFG and ACC.

The results further indicated significant positive effective coupling between the left IFG (seed region) and DLPFC, DMPFC, right MTG and STG during down-regulation of emotion depending on reappraisal success (Table 4). Figure 4C illustrates the positive correlation between effective connectivity beta estimates for the left IFG and SFG and 'Decrease' success. In contrast, a negative correlation between effective connectivity and 'Decrease' success was found between left IFG (seed region) and right IFG, left SFG/VMPFC and left orbital gyrus (Table 4). Figure 4D illustrates the negative correlation between effective connectivity beta estimates for the left IFG (and left SFG/VMPFC) and 'Decrease' success.

Left amygdala seed region. The PPI analysis based on the left amygdala as seed region demonstrated a positive correlation between 'Increase' success and the coupling with a number of regions such as left IFG, left MFG, left SFG, subgenual ACC (sgACC), left STG, left insula, left IPL, left MTG and left parahippocampal gyrus (Table 5). Figure 5A illustrates the positive correlation between successful up-regulation of emotion and effective coupling of the left amygdala (seed region) with left IFG. Effective connectivity between the left amygdala (seed region) and the right SFG/OFC was negatively correlated with 'Increase' success, illustrated in Figure 5B and reported in Table 5.

The activity in the left amygdala was positively correlated with activity in the bilateral fusiform gyri, right parahippocampal gyrus and occipital cortex and 'Decrease' success (Table 5). We also found a negative correlation between 'Decrease' success and the effective coupling between the left amygdala and the right precuneus.

In summary, we found that the down-regulation of emotion was associated with increased effective connectivity in a prefrontal network, including the left VLPFC, DLPFC and DMPFC, depending on reappraisal success (Figure 6A). Furthermore, decreased coupling between left IFG and VMPFC during the down-regulation of emotion was correlated with greater reappraisal success. Up-regulation of emotion was based on

Table 5. Task-related PPI analysis with success scores as covariate for left amygdala seed region

Region	BA	Side	Coordinates			Voxels	t-value
			x	y	z		
'Decrease>Look Negative with Decrease success as covariate'							
Lingual Gyrus	18	RH	6	−88	−11	447	0.71
Middle occipital gyrus	19	RH	30	−91	16	LM	0.67
Inferior occipital gyrus	17	RH	18	−91	−5	LM	0.61
Fusiform gyrus	19	RH	24	−82	−14	LM	0.60
Inferior occipital gyrus	18	LH	−30	−91	−2	293	0.63
Fusiform gyrus	19	LH	−39	−76	−11	LM	0.63
Lingual gyrus	18	LH	−18	−97	−11	LM	0.62
Fusiform gyrus	37	RH	36	−43	−11	99	0.63
Parahippocampal gyrus	36	RH	36	−34	−14	LM	0.56
Precuneus	7	RH	30	−46	52	98	−0.60
Precuneus	7	RH	15	−61	49	LM	−0.54
'Increase>Look Negative with Increase success as covariate'							
IFG/VLPFC	47	LH	−33	17	−11	1542	0.71
STG	22	LH	−45	−10	−5	LM	0.67
Insula	13	LH	−39	−25	16	LM	0.64
IFG	47	LH	−30	32	−2	LM	0.64
Inferior parietal lobule	40	LH	−48	−31	22	LM	0.63
Pre-central gyrus	4	LH	−51	−10	25	LM	0.62
Middle temporal gyrus	19	LH	−39	−61	13	LM	0.62
Insula	13	LH	−33	26	13	LM	0.60
Post-central gyrus	2	LH	−36	−25	28	LM	0.60
Inferior temporal gyrus	21	LH	−60	−13	−17	LM	0.59
Post-central gyrus	43	LH	−63	−10	16	LM	0.55
Caudate		LH	−30	−37	4	LM	0.55
Parahippocampal gyrus	36	LH	−24	−37	−8	LM	0.52
Lentiform nucleus		LH	−27	2	10	LM	0.51
STG	22	LH	−57	−43	13	LM	0.50
STG	39	LH	−39	−58	31	LM	0.45
MFG/DLPFC	9	LH	−42	11	34	498	0.71
MFG	6	LH	−24	8	43	LM	0.65
medFG	8	RH	12	38	40	LM	0.64
SFG	8	LH	−9	41	43	LM	0.63
medFG	8	LH	−12	26	46	LM	0.60
medFG	6	LH	−15	29	37	LM	0.60
Anterior cingulate	32	RH	12	38	25	LM	0.58
Anterior cingulate	32	LH	−3	38	19	LM	0.52
Middle temporal gyrus	21	RH	63	−40	−14	1255	0.67
Lentiform nucleus		RH	33	−16	1	LM	0.65
Middle temporal gyrus	21	RH	60	−22	−8	LM	0.63
Insula	13	RH	45	−16	22	LM	0.61
Middle temporal gyrus	21	RH	57	−40	1	LM	0.61
Thalamus		RH	21	−34	1	LM	0.59
Midbrainred nucleus		LH	0	−16	−2	LM	0.57
STG	22	RH	48	−1	1	LM	0.57
STG		RH	66	−25	1	LM	0.57
STG	22	RH	66	−40	10	LM	0.56
Middle temporal gyrus	37	RH	42	−58	4	LM	0.56
Transverse temporal gyrus		RH	57	−13	10	LM	0.55
Midbrainred nucleus		LH	0	−25	−8	LM	0.55
STG	22	RH	48	−22	−11	LM	0.54
Post-central gyrus	2	RH	60	−22	34	LM	0.54
STG	42	RH	66	−25	16	LM	0.51
STG	39	RH	45	−52	19	LM	0.51
Anterior cingulate	24	RH	3	35	7	133	0.66
medFG/DMPFC	10	LH	−12	50	7	LM	0.63
MFG/DMPFC	10	LH	−24	50	4	LM	0.58
Post-central gyrus	3	LH	−18	−37	70	165	0.65
Post-central gyrus	1	LH	−33	−34	64	LM	0.62
Post-central gyrus	2	LH	−42	−28	52	LM	0.52
Posterior cingulate	23	RH	3	−34	16	244	0.56
Cingulate gyrus	31	LH	−15	−49	19	LM	0.56
Posterior cingulate	30	LH	−6	−52	13	LM	0.55
SFG/OFC	11	RH	27	53	−20	117	−0.67
SFG/OFC	11	RH	18	53	−17	LM	−0.63

LM, local maxima.

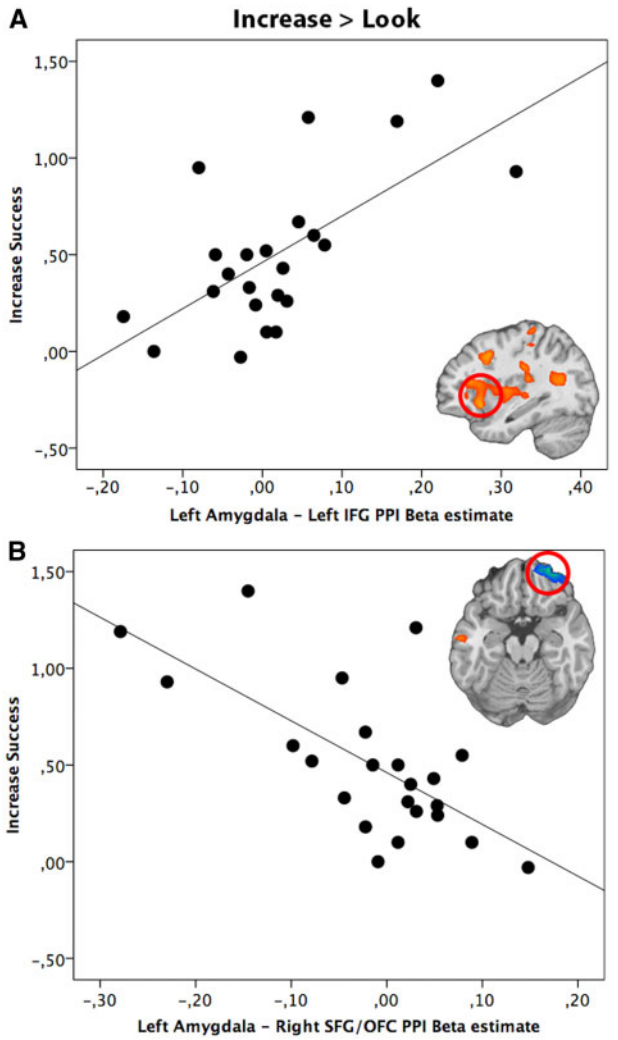

Fig. 5. Relationship between reappraisal success scores (Increase Success) and PPI beta estimate of left amygdala coupling with **(A)** left IFG and **(B)** right SFG (SFG/OFC) during the up-regulation of emotion (Increase > Look). The scatter plot is solely for illustrative purposes (e.g. to show the absence of outliers), and is not used for statistical inference.

increased effective connectivity between the left IFG and VMPFC and correlated positively with reappraisal success (Figure 6B). A negative correlation between reappraisal success and connectivity of the left IFG with the DMPFC and pgACC during the up-regulation of emotion was observed. Moreover, increased effective coupling between the IFG with the amygdala correlating positively with reappraisal success was found for the 'Increase' condition. The amygdala was further coactivated with the sgACC, DLPFC and DMPFC and this coupling was predicted by higher reappraisal success when up-regulating emotions. In contrast, there was a negative relationship between reappraisal success during the up-regulation of emotional responses and the coupling between the amygdala with the OFC. These results indicate that emotion regulation was based on amygdala-prefrontal interactions that were tightly linked to the ability to successfully regulate emotions.

Discussion

Previous studies on reappraisal indicated that VLPFC, in particular the IFG, and the amygdala serve different key functional roles in the reappraisal process (Eippert *et al.*, 2007; Wager *et al.*, 2008). However, the effective coupling between VLPFC and amygdala with other regions of the brain during reappraisal and their association with reappraisal success is unclear. The present work constitutes the first investigation into this question by explicitly including reappraisal success as a regressor in the connectivity model.

In our reappraisal task, subjects had to either up- or down-regulate their emotions in response to aversive pictures. The effect of emotion regulation was demonstrated on the behavioral, psychophysiological and neural level. First, during emotion regulation subjects rated their emotional state as either increased or decreased according to the reappraisal condition compared with the control condition. Second, SCRs were increased during the up-regulation compared with the down-regulation of emotion (Eippert *et al.*, 2007; Urry *et al.*, 2009; Morawetz *et al.*, 2016b,c). Third, in accord with previous findings, reappraisal compared with the control condition was associated with enhanced responses in VLPFC, temporal and parietal regions as well as the amygdala (Urry *et al.*, 2006; Eippert *et al.*, 2007; Kim and Hamann, 2007; Buhle *et al.*, 2014; Frank *et al.*, 2014; Kohn *et al.*, 2014; Morawetz *et al.*, 2016c). We therefore conclude that our paradigm was suited to investigate the effect of emotion regulation on connectivity and its relation to reappraisal success.

Prefrontal network underlying the down-regulation of emotion

No study to date has used the IFG as seed region for a connectivity analysis in the context of emotion regulation. This is surprising since the left IFG has been implicated in response selection and inhibition, language, social cognition and inner speech during the emotion regulation process (Ochsner *et al.*, 2012; Kohn *et al.*, 2014; Messina *et al.*, 2015). Here we found that increased effective coupling between the left IFG and dorsal prefrontal regions (DMPFC and DLPFC) was associated with reappraisal success during the down-regulation of emotional responses. In a previous study, we found that emotion regulation was mediated by directional changes of connection strength between the IFG and DLPFC (Morawetz *et al.*, 2016c). We now demonstrate that the ability to successfully regulate ones emotions was predicted by an enhanced effective connectivity between those two prefrontal regions. This indicates that the suggested feedback mechanism between DLPFC and IFG during emotion regulation (Morawetz *et al.*, 2016c) might be more prominent in individuals possessing higher reappraisal skills. Within this frontal network, DMPFC appears to play a critical role in emotion regulation as it has repeatedly been shown to be involved in various aspects of reflective emotional processing (Phan *et al.*, 2002). This region has been suggested to be implicated in the control of emotional behaviors and to relay internal state information to the DLPFC and VLPFC via a feed-forward mechanism (Phillips *et al.*, 2008).

Interestingly, we found a negative correlation between IFG-VMPFC coupling and down-regulation success, while the reverse pattern was found for the up-regulation of emotion. These findings are closely aligned with the view that VMPFC plays a key role in conceptually driven affect (Roy *et al.*, 2012). Reappraisal as a conceptually-driven form of emotion regulation, i.e. with the goal to generate positive ('Decrease') or negative ('Increase') conceptual frames, has previously been linked to VMPFC activity (Diekhof *et al.*, 2011). Previous imaging studies also implicated the VMPFC in the positive and negative

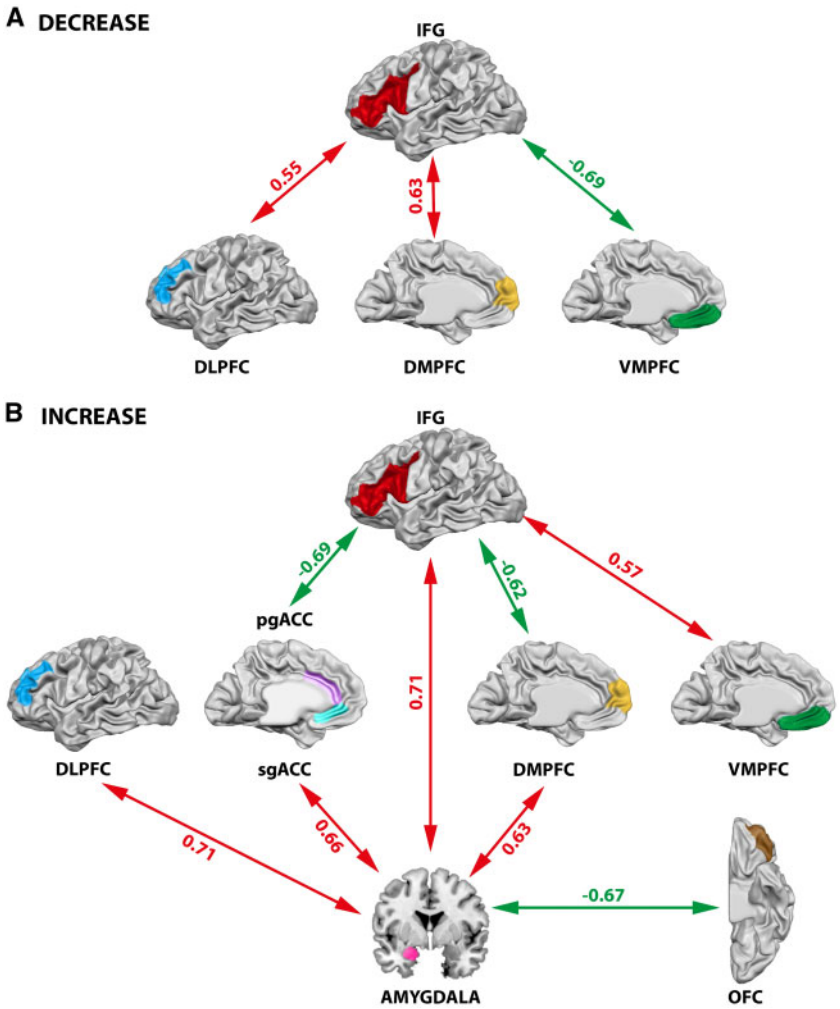

Fig. 6. Illustration of the results of the PPI-analyses with focus on prefrontal-subcortical interactions. Red arrows indicate a positive correlation between the effective coupling of two regions and reappraisal success, while green arrows indicate a negative correlation between the effective coupling of two regions and reappraisal success. **(A)** Prefrontal network observed during the down-regulation (Decrease) of emotion. **(B)** Amygdalaprefrontal network observed during the up-regulation (Increase) of emotion. IFG, inferior frontal gyrus; DLPFC, dorsolateral prefrontal cortex; DMPFC, dorsomedial prefrontal cortex; VMPFC, ventromedial prefrontal cortex; pgACC, pregenual anterior cingulate cortex; sgACC, subgenual anterior cingulate cortex; OFC, orbitofrontal cortex. *t*-values for each connection are reported.

valuation of stimuli in a context- and goal-dependent manner (Hare *et al.*, 2009; Hutcherson *et al.*, 2012). Our results show that the successful reframing of negative stimuli in a positive direction (i.e. decreasing emotions to feel less negative affect) was related to less effective coupling between IFG and VMPFC. In contrast, the successful reframing of aversive pictures in a negative direction (i.e. increasing emotions to feel more negative affect) was associated with enhanced effective connectivity between IFG and VMPFC. These findings indicate that the up-regulation of emotion might be more cognitively demanding which could lead to the stronger subsequent recruitment of the VMPFC. In the opposite scenario, it might be easier to develop appropriate positive concepts to down-regulate emotions, and this process might therefore be associated with less effective coupling between IFG and VMPFC.

Of note, the observed network is based on the IFG as seed region because this prefrontal region has been directly linked to reappraisal success in previous studies (see 'Materials and methods' section). However, it might be worthwhile to use other prefrontal regions as seed regions if there is an indication that this region is related to successful emotion regulation. In the present study we used a hypothesis-driven analysis approach and only considered brain regions for which clear evidence for a direct link to emotion regulation success was given.

Amygdala-prefrontal network underlying the up-regulation of emotion

Consistent with previous findings (Banks *et al.*, 2007) we found that increased connectivity between the left amygdala and OFC was associated with the experience of less negative affect. In addition, we extended previous studies (Banks *et al.*, 2007; Kanske *et al.*, 2011; Sripada *et al.*, 2014) by showing that several other prefrontal regions (VLPFC, DLPFC, DMPFC and sgACC) demonstrated increased coupling with the amygdala with increasing success in up-regulating emotions.

The reappraisal-modulated coactivation of amygdala and IFG with ACC with respect to regulating negative affect is in line with prior neuroimaging results that implicate the ACC in emotion assessment, emotion related learning, and active, voluntary emotion regulation (Ochsner and Gross, 2005; Phillips *et al.*,

2008; Wager *et al.*, 2008; Etkin *et al.*, 2011; Ochsner *et al.*, 2012; Stevens *et al.*, 2012). We observed a differential connectivity profile for the ACC during the up-regulation of emotion: Increased coupling between sgACC and amygdala predicted increased reappraisal success, while decreased coupling between pgACC and IFG predicted less reappraisal success. The increased coupling between the IFG and pgACC and its negative association with reappraisal success might represent a form of successful emotional conflict resolution (Beauregard *et al.*, 2001; Etkin *et al.*, 2006): when participants were unable to up-regulate their negative emotions, this might have led to less emotional conflict and thus less effective coupling between IFG and pgACC. In support, the sgACC has been found to be activated when participants were asked to attend to core affective feelings and rate their feelings (Lindquist *et al.*, 2012). Consistent with this view, reappraisal-related sgACC activation has been interpreted to signify self-relevant processing or focus on one's feelings (Kross *et al.*, 2009; Urry *et al.*, 2009). This implies that the observed positive association between reappraisal success and increased coupling between the amygdala with sgACC might indicate heightened monitoring of internal emotional states (Abler *et al.*, 2008).

Our findings suggest that the successful down-regulation of emotions predicted increased coupling of prefrontal regions, while the successful up-regulation of emotional experience was related to increased coupling of amygdala-prefrontal interactions. The discrepancy to previous studies (Urry *et al.*, 2006; Banks *et al.*, 2007; Kanske *et al.*, 2011) reporting amygdala-frontal coupling during the down-regulation of emotion might be explained by individual differences in reappraisal success. To test this hypothesis, we performed the same PPI analysis with the left amygdala as seed region 'without' using reappraisal success as covariate. Consistent with the notion that frontal cortex exerts a top-down inhibitory effect on the amygdala (Ochsner *et al.*, 2002; Quirk and Beer, 2006; Urry *et al.*, 2006; Johnstone *et al.*, 2007; Phillips *et al.*, 2008; Wager *et al.*, 2008), we found that increased activity in bilateral VLPFC was associated with decreased activity in the left amygdala during the down-regulation of negative affect. In contrast, an increase in response in the left VLPFC was associated with an increase in signal change in the amygdala during the up-regulation of emotions (see Supplementary Table S1). This supports the idea that individual differences in reappraisal success might affect amygdala-frontal coupling during the down-regulation of emotion.

Furthermore, amygdala-frontal coupling might also be affected by reappraisal training. Recent findings indicate that reappraisal training, i.e. increasing reappraisal success, not only results in reductions in self-reported negative affect over time (Denny and Ochsner, 2014), but also leads to long-lasting effects on the amygdala response (Denny *et al.*, 2015). In line with these findings, previous studies demonstrated that neurofeedback training leads to an increase in top-down connectivity from the DMPFC onto the amygdala (Koush *et al.*, 2015) as well as in bottom-up connectivity from the amygdala to the VMPFC (Paret *et al.*, 2016). These findings indicate that the amygdala-frontal coupling underlying successful emotion regulation can be modulated in a self-organized, endogenous fashion. Furthermore, the coupling within cortico-limbic circuits can also be influenced pharmacologically by targeting the serotonergic system, which has been implicated in a wide range of psychiatric diseases, in particular in anxiety disorders and depression. Serotonin has been linked to several aspects of emotional information processing (Merens *et al.*, 2007) and thus might be implicated in amygdala-frontal coupling. Indeed, a recent study demonstrated that effective connectivity within the prefrontal-amygdala network can be modulated by (S)-citalopram, a selective serotonin reuptake inhibitor, during emotional face processing (Sladky *et al.*, 2015). Hence, the proposed emotion regulation network could not only be modulated on a behavioral, but also on a neuropharmacological level.

Conclusions

Our findings have several implications, first by providing further evidence for the importance of frontal brain regions to regulate emotions. Furthermore, these findings add to prior neuroimaging studies by showing that up- and down-regulation of emotions are based on different coupling between prefrontal regions and the amygdala. Increased coupling within a prefrontal network was related to success in down-regulation of emotions, and increased coupling between the amygdala and the prefrontal network was related to success in the up-regulation of emotions. They additionally suggest that there is a direct link between effective connectivity underlying emotion regulation and the success in controlling emotions thereby highlighting the role of individual differences. In relation to conceptual models of emotion regulation (Ochsner *et al.*, 2012), the findings demonstrate that successful reappraisal might rely on a more direct interaction between a system involved in the control of emotions based on frontal regions and a system implicated in generating emotions involving emotion-related regions such as the amygdala. Finally, given that psychiatric disorders have been found to be associated with affective instability and emotion dysregulation (Phillips *et al.*, 2003), our findings might inform future studies investigating whether specific connectivity deficits could underlie emotion regulation deficits in mental disorders, such as anxiety, mood and personality disorders.

Supplementary data

Supplementary data are available at *SCAN* online.

Conflict of interest. None declared.

References

Abler, B., Hofer, C., Viviani, R. (2008). Habitual emotion regulation strategies and baseline brain perfusion. *Neuroreport*, **19**, 21–4.

Amaral, D.G., Price, J.L. (1984). Amygdalo-cortical projections in the monkey (Macaca fascicularis). *Journal of Comparative Neurology*, **230**, 465–96.

Amstadter, A. (2008). Emotion regulation and anxiety disorders. *Journal of Anxiety Disorders*, **22**, 211–21.

Banks, S.J., Eddy, K.T., Angstadt, M., Nathan, P.J., Phan, K.L. (2007). Amygdala-frontal connectivity during emotion regulation. *Social Cognitive and Affective Neuroscience* **2**, 303–12.

Barbas, H. (2000). Connections underlying the synthesis of cognition, memory, and emotion in primate prefrontal cortices. *Brain Research Bulletin* **52**, 319–30.

Barbas, H. 2009. Prefrontal cortex: structure and anatomy. In: Squire, L., editor. *Encyclopedia of Neuroscience, pp. 909–18*. Oxford: Academic Press.

Barbas, H., Pandya, D.N. (1989). Architecture and intrinsic connections of the prefrontal cortex in the rhesus monkey. *Journal of Comparative. Neurology*, **286**, 353–75.

Barbas, H., Pandya, N. 1991. Patterns of connections of the prefrontal cortex in the rhesus monkey associated with cortical

architecture. In: Levin, H., Eisenberg, H., Benton, A., editors. *In Frontal Lobe Function and Dysfunction, pp. 35–58*. New York: Oxford University Press.

Beauregard, M., Lévesque, J., Bourgouin, P. (2001). Neural correlates of conscious self-regulation of emotion. *Journal of Neuroscience*, **21**, RC165.

Benedek, M., Kaernbach, C. (2010a). Decomposition of skin conductance data by means of nonnegative deconvolution. *Psychophysiology*, **47**, 647–58.

Benedek, M., Kaernbach, C. (2010b). A continuous measure of phasic electrodermal activity. *Journal of Neuroscience Methods*, **190**, 80–91.

Bennett, C.M., Wolford, G.L., Miller, M.B. (2009). The principled control of false positives in neuroimaging. *Social Cognitive and Affective Neuroscience*, **4**, 417–22.

Berking, M., Wupperman, P. (2012). Emotion regulation and mental health: recent findings, current challenges, and future directions. *Current Opinion in Psychiatry*, **25**, 128–34.

Bradley, M., Miccoli, L., Escrig, M., Lang, P. (2008). The pupil as a measure of emotional arousal and autonomic activation. *Psychophysiology*, **45**, 602–7.

Bradley, M.M., Lang, P.J. 2007. The International Affective Picture System (IAPS) in the study of emotion and attention. In: Coan, J.A., Allen, J.J., editors. *Handbook of Emotion Elicitation and Assessment, Series in Affective Science, pp. 29–46*. New York: Oxford University Press.

Buhle, J.T., Silvers, J. a., Wager, T.D., *et al.* (2014). Cognitive reappraisal of emotion: a meta-analysis of human neuroimaging studies. *Cerebral Cortex*, **24**, 2981–90.

Cisler, J.M., Olatunji, B.O., Feldner, M.T., Forsyth, J.P. (2010). Emotion Regulation and the Anxiety Disorders: An Integrative Review. *Journal of. Psychopathology and Behavioral Assessment*, **32**, 68–82.

Davidson, R.J. (2000). Dysfunction in the neural circuitry of emotion regulation–a possible prelude to violence. *Science*, **289**, 591–4.

Denny, B.T., Inhoff, M.C., Zerubavel, N., Davachi, L., Ochsner, K.N. (2015). Getting over it: long-lasting effects of emotion regulation on amygdala response. *Psychological Science*, **26**, 1377–88.

Denny, B.T., Ochsner, K.N. (2014). Behavioral effects of longitudinal training in cognitive reappraisal. *Emotion*, **14**, 425–33.

Diekhof, E.K., Geier, K., Falkai, P., Gruber, O. (2011). Fear is only as deep as the mind allows: a coordinate-based meta-analysis of neuroimaging studies on the regulation of negative affect. *Neuroimage* **58**, 275–85.

Eftekhari, A., Zoellner, L.A., Vigil, S.A. (2009). Patterns of emotion regulation and psychopathology. *Anxiety Stress Coping*, **22**, 571–86.

Eickhoff, S.B., Stephan, K.E., Mohlberg, H. *et al.* (2005). A new SPM toolbox for combining probabilistic cytoarchitectonic maps and functional imaging data. *Neuroimage*, **25**, 1325–35.

Eippert, F., Veit, R., Weiskopf, N., Erb, M., Birbaumer, N., Anders, S. (2007). Regulation of emotional responses elicited by threat-related stimuli. *Humand Brain Mapping*, **28**, 409–23.

Etkin, A., Egner, T., Kalisch, R. (2011). Emotional processing in anterior cingulate and medial prefrontal cortex. *Trends in Cognitive Science*, **15**, 85–93.

Etkin, a., Egner, T., Peraza, D., Kandel, E., Hirsch, J. (2006). Resolving emotional conflict: a role for the rostral anterior cingulate cortex in modulating activity in the amygdala. *Neuron*, **51**, 871–82.

Forman, S.D., Cohen, J.D., Fitzgerald, M., Eddy, W.F., Mintun, M.A., Noll, D.C. (1995). Improved assessment of significant activation in functional magnetic resonance imaging (fMRI): use of a cluster-size threshold. *Magnetic Resonance in Medicine*, **33**, 636–47.

Frank, D.W., Dewitt, M., Hudgens-Haney, M., *et al.* (2014). Emotion regulation: quantitative meta-analysis of functional activation and deactivation. *Neuroscience and Biobehavioral Reviews*, **45**, 202–11.

Friston, K., Buechel, C., Fink, G., Morris, J., Rolls, E., Dolan, R. (1997). Psychophysiological and modulatory interactions in neuroimaging. *Neuroimage*, **6**, 218–29.

Friston, K.J. (2011). Functional and effective connectivity: a review. *Brain Connect*, **1**, 13–36.

Friston, K.J., Harrison, L., Penny, W. (2003). Dynamic causal modelling. *Neuroimage*, **19**, 1273–302.

Ghashghaei, H.T., Barbas, H. (2002). Pathways for emotion: interactions of prefrontal and anterior temporal pathways in the amygdala of the rhesus monkey. *Neuroscience*, **115**, 1261–79.

Ghashghaei, H.T., Hilgetag, C.C., Barbas, H. (2007). Sequence of information processing for emotions based on the anatomic dialogue between prefrontal cortex and amygdala. *Neuroimage*, **34**, 905–23.

Goulas, A., Stiers, P., Uylings, H.B.M. (2012). Unravelling the Intrinsic Functional Organization of the Human Lateral Frontal Cortex: A Parcellation Scheme Based on Resting State fMRI. *Journal of. Neuroscience*, **32**, 10238–52.

Gross, J.J., Muñoz, R.F. (1995). Emotion regulation and mental health. *Clinical Psychology: Sciecne and Practice*, **2**, 151–64.

Gross, J.J., Richards, J.M., John, O.P. 2006. Emotion regulation in everyday life. In: Snyder, D.K., Simpson, J.A., Hughes, J.N., editors. *Emotion Regulation in Couples and Families: Pathways to Dysfunction and Health*, pp. 13–35. Washington, DC: American Psychological Association.

Gross, J.J., Thompson, R.A. 2007. Emotion regulation: conceptual foundations. In: Gross, J.J., editor. *Handbook of Emotion Regulation*, pp. 3–24. New York: Guilford Press.

Gruber, J., Harvey, A.G., Gross, J.J. (2012). When trying is not enough: emotion regulation and the effort-success gap in bipolar disorder. *Emotion*, **12**, 997–1003.

Hare, T. a., Camerer, C.F., Rangel, A. (2009). Self-control in decision-making involves modulation of the vmPFC valuation system. *Science*, **324**, 646–8.

Hutcherson, C. a., Plassmann, H., Gross, J.J., Rangel, A. (2012). Cognitive regulation during decision making shifts behavioral control between ventromedial and dorsolateral prefrontal value systems. *Journal of Neuroscience*, **32**, 13543–54.

Johnstone, T., van Reekum, C.M., Urry, H.L., Kalin, N.H., Davidson, R.J. (2007). Failure to regulate: counterproductive recruitment of top-down prefrontal-subcortical circuitry in major depression. *Journal of Neuroscience* **27**, 8877–84.

Kalisch, R. (2009). The functional neuroanatomy of reappraisal: time matters. *Neuroscience and Biobehavioral Reviews*, **33**, 1215–26.

Kanske, P., Heissler, J., Schönfelder, S., Bongers, A., Wessa, M. (2011). How to regulate emotion? Neural networks for reappraisal and distraction. *Cerebral Cortex*, **21**, 1379–88.

Kim, S.H., Hamann, S. (2007). Neural correlates of positive and negative emotion regulation. *Journal of Cognitvie Neuroscience*, **19**, 776–98.

Kohn, N., Eickhoff, S.B., Scheller, M., Laird, a. R., Fox, P.T., Habel, U. (2014). Neural network of cognitive emotion regulation - an ALE meta-analysis and MACM analysis. *Neuroimage*, **87**, 345–55.

Koush, Y., Meskaldji, D.E., Pichon, S. *et al.* (2015). Learning control over emotion networks through connectivity-based neurofeedback. *Cerebral Cortex*, **17**. doi:10.1093/cercor/bhv311.

Krause-Utz, A., Winter, D., Niedtfeld, I., Schmahl, C. (2014). The latest neuroimaging findings in borderline personality disorder. *Current Psychiatry Reports*, **16**, 438.

Kross, E., Davidson, M., Weber, J., Ochsner, K. (2009). Coping with emotions past: the neural bases of regulating affect associated with negative autobiographical memories. *Biological Psychiatry*, **65**, 361–6.

Lindquist, K. a., Wager, T.D., Kober, H., Bliss-Moreau, E., Barrett, L.F. (2012). The brain basis of emotion: a meta-analytic review. *Behavioral and. Brain Sciences*, **35**, 121–43.

Lohmann, G., Erfurth, K., Müller, K., Turner, R. (2012). Critical comments on dynamic causal modelling. *Neuroimage*, **59**, 2322–9.

Merens, W., Willem Van der Does, A.J., Spinhoven, P. (2007). The effects of serotonin manipulations on emotional information processing and mood. *Journal of Affective Disorders*, **103**, 43–62.

Messina, I., Bianco, S., Sambin, M., Viviani, R. (2015). Executive and semantic processes in reappraisal of negative stimuli: insights from a meta-analysis of neuroimaging studies. *Frontiers in Psychology*, **6**, 974–83.

Morawetz, C., Alexandrowicz, R.W., Heekeren, H.R. 2016. *Successful emotion regulation is predicted by amygdala activity and aspects of personality: A latent variable approach*. Emotion November 7.

Morawetz, C., Bode, S., Baudewig, J., Jacobs, A.M., Heekeren, H.R. (2016b). Neural representation of emotion regulation goals. *Human Brain Mapping* **37**, 600–20.

Morawetz, C., Bode, S., Baudewig, J., Kirilina, E., Heekeren, H.R. (2016c). Changes in effective connectivity between dorsal and ventral prefrontal regions moderate emotion regulation. *Cerebral Cortex*, **26**, 1923–37.

Ochsner, K.N., Bunge, S.A., Gross, J.J., Gabrieli, J.D.E. (2002). Rethinking feelings: an fmri study of the cognitive regulation of emotion. *J. Cognitive Neuroscience*, **14**, 1215–29.

Ochsner, K.N., Gross, J.J. (2005). The cognitive control of emotion. *Trends in Cognitive Science*, **9**, 242–9.

Ochsner, K.N., Ray, R.D., Cooper, J.C., *et al.* (2004). For better or for worse: neural systems supporting the cognitive down- and up-regulation of negative emotion. *Neuroimage*, **23**, 483–99.

Ochsner, K.N., Silvers, J., Buhle, J.T. (2012). Functional imaging studies of emotion regulation: a synthetic review and evolving model of the cognitive control of emotion. *Annals of the New York Academy of Sciences*, **1251**, E1–24. doi:10.1111/j.1749-6632.2012.06751.x.

Oldfield, R.C. (1971). The assessment and analysis of handedness: the Edinburgh inventory. *Neuropsychologia*, **9**, 97–113.

Paret, C., Ruf, M., Gerchen, M.F., *et al.* (2016). FMRI neurofeedback of amygdala response to aversive stimuli enhances prefrontal-limbic brain connectivity. *Neuroimage*, **125**, 182–8.

Payer, D.E., Baicy, K., Lieberman, M.D., London, E.D. (2012). Overlapping neural substrates between intentional and incidental down-regulation of negative emotions. *Emotion*, **12**, 229–35.

Phan, K.L., Wager, T., Taylor, S.F., Liberzon, I. (2002). Functional neuroanatomy of emotion: a meta-analysis of emotion activation studies in PET and fMRI. *Neuroimage*, **16**, 331–48.

Phillips, M.L., Drevets, W.C., Rauch, S.L., Lane, R. (2003). Neurobiology of emotion perception II: Implications for major psychiatric disorders. *Biological Psychiatry*, **54**, 515–28.

Phillips, M.L., Ladouceur, C.D., Drevets, W.C. (2008). A neural model of voluntary and automatic emotion regulation: implications for understanding the pathophysiology and neurodevelopment of bipolar disorder. *Molecular Psychiatry*, **13**, 829–57.

Quirk, G.J., Beer, J.S. (2006). Prefrontal involvement in the regulation of emotion: convergence of rat and human studies. *Current Opinion in Neurobiology*, **16**, 723–7.

Ray, R.D., Zald, D.H. (2012). Anatomical insights into the interaction of emotion and cognition in the prefrontal cortex. *Neuroscience and Biobehavioral Reviews*, **36**, 479–501. doi:10.1016/j.neubiorev.2011.08.005.

Roy, M., Shohamy, D., Wager, T.D. (2012). Ventromedial prefrontal-subcortical systems and the generation of affective meaning. *Trends in Cognitive Science*, **16**, 147–56.

Sergerie, K., Chochol, C., Armony, J.L. (2008). The role of the amygdala in emotional processing: a quantitative meta-analysis of functional neuroimaging studies. *Neuroscience and Biobehavioral Reviews*, **32**, 811–30.

Sladky, R., Spies, M., Hoffmann, A., *et al.* (2015). (S)-citalopram influences amygdala modulation in healthy subjects: a randomized placebo-controlled double-blind fMRI study using dynamic causal modeling. *Neuroimage*, **108**, 243–50.

Sripada, C., Angstadt, M., Kessler, D., *et al.* (2014). Volitional regulation of emotions produces distributed alterations in connectivity between visual, attention control, and default networks. *Neuroimage*, **89**, 110–21.

Stevens, F.L., Hurley, R.A., Taber, K.H. (2012). Anterior cingulate cortex: unique role in cognition and emotion. *Journal of Clinical Neuroscience*, **23**, 2–6.

Talairach, J., Tournoux, P. 1988. *Co-Planar Stereotaxic Atlas of the Human Brain (Thieme Classics)*. Stuttgart: Thieme.

Urry, H.L., Reekum, V., Marije, C., *et al.* (2006). Amygdala and ventromedial prefrontal cortex are inversely coupled during regulation of negative affect and predict the diurnal pattern of cortisol secretion among older adults. *Journal of Neuroscience*, **26**, 4415–25.

Urry, H.L., van Reekum, C.M., Johnstone, T., Davidson, R.J. (2009). Individual differences in some (but not all) medial prefrontal regions reflect cognitive demand while regulating unpleasant emotion. *Neuroimage*, **47**, 852–63.

Wager, T.D., Davidson, M.L., Hughes, B.L., Lindquist, M.A., Ochsner, K.N. (2008). Prefrontal-subcortical pathways mediating successful emotion regulation. *Neuron*, **59**, 1037–50.

Yeterian, E.H., Pandya, D.N., Tomaiuolo, F., Petrides, M. (2012). The cortical connectivity of the prefrontal cortex in the monkey brain. *Cortex*, **48**, 58–81.

Zald, D.H. (2003). The human amygdala and the emotional evaluation of sensory stimuli. *Brain Research Reviews*, **41**, 88–123.

Zelazo, P.D., Cunningham, W.A. 2007. Executive function: Mechanisms underlying emotion regulation. In: Gross, J., editor. *Handbook of Emotion Regulation*, pp. 135–158. New York: Guilford.